Progress In Electromagnetics Research, PIER 72, 47–59, 2007

A NEW INTERPOLATION TECHNIQUE FOR THE RECONSTRUCTION OF UNIFORMLY SPACED SAMPLES FROM NON-UNIFORMLY SPACED ONES IN PLANE-RECTANGULAR NEAR-FIELD ANTENNA MEASUREMENTS

V. Dehghanian

Department of Electrical Engineering
Islamic Azad University-Garmsar Branch
Garmsar, Iran

M. Okhovvat

Imam Hussain University
Tehran, Iran

M. Hakkak

Department of Electrical Engineering
Tarbiat Modares University
Tehran, Iran

Abstract—A novel fast and accurate interpolation technique for recovering the uniformly distributed samples from the irregularly spaced samples, collected non-uniformly due to the probe position error in planar near-field antenna measurements, is presented. The technique employs Yen's interpolator and tries to make it as practical as possible for the use in near-field antenna measurements. A comprehensive simulation capability is developed and through out the simulations the speed and precision of this accurate and timely efficient interpolation technique is compared with some other techniques which are also based on Yen's interpolators. The results well demonstrate the advantages of our technique we termed "The Cross-Rail Technique".

1. INTRODUCTION

Near-field antenna measurement techniques are traditionally divided into planar, cylindrical, and spherical techniques, where each has its own particular advantages, depending upon the antenna under test, AUT, and the measurement requirements [1]. Recently, a new technique based on spiral scanning has been described [2]. The planar near-field techniques can be further subdivided into plane-rectangular, plane-polar, and bipolar technique. All of the near-field measurement techniques rely heavily on data processing of measured data. However, the planar techniques are of more practical interest since they employ rather simple scanners. Also NF to FF transformation for planar techniques is of less order of time complexity, comparing to those of cylindrical or spherical techniques. Among planar techniques the plane-rectangular (PR) configuration is the most-common near-field scanner in use today. In this technique a raster scanning of the probe produces planar measurement samples on a regular rectangular grid in Cartesian coordinates. These uniformly distributed samples can be processed into the far-field using an FFT algorithm [3]. A. C. Newell [4] has identified 18 error sources in the planar near-field measurement. Three of them are directly related to alignment or position error associated with the probe or the AUT. Position accuracy for near-field measurements will vary depending upon the test requirements. However an accuracy of $\lambda/100$ is considered adequate for most application. For an L-band antenna this represents an accuracy requirement of approximately 6.3 mm, and for Ku-band 0.075 mm is required. Near-field scanners have been operated for as high as 550 GHz requiring an accuracy of 0.005 mm [5]. For these antennas, careful attention to the design and construction of the near-field scanner is essential, though not enough. Special error correction techniques are necessary to achieve this level of accuracy [6]. Also, some phase delay and phase velocity aspects in the near-field measurements have to be observed [7].

Although uniform sampling techniques can be used in a variety of situations, there are many circumstances for which it may not be practical to directly utilize uniform sampling techniques, i.e., when one performs antenna measurements for which it may not be possible to control the antenna or probe movements to the desired locations in space. One example is the measurement of large antennas aboard the space shuttles. Similar situations may also occur for the in-orbit measurement of satellite antennas using ground-based terminals [8]. In order to predict the far-field from the non-uniformly distributed near-field samples in planar near-field antenna measurements, two necessary

steps shall be taken. First, a two-dimensional optimal-sampling-interpolation (OSI) is to be deployed to reconstruct the near-field data in a regular rectangular grid. Subsequently, the FFT algorithm shall be utilized to predict the far-field.

The problem of signal reconstruction from non-uniformly spaced data can be found in various contexts. Many types of interpolation algorithms have been devised for reconstruction of band-limited signals from non-uniform samples. But the most accurate interpolation algorithm was first derived by Yen [9].

Although Yen's interpolation algorithm is best in theory, practically there are severe difficulties in computing the interpolated values numerically such as the very high computer time and the ill condition phenomenon of $Q^2 \times Q^2$ matrix (Q^2 is the number of samples) especially for cases with high quantity of samples [10]. Efforts have been made in order to decrease the time complexity of Yen's interpolation algorithm [10–13]. In this paper we introduce an optimal fast and simple interpolation technique for the reconstruction of regularly spaced samples from the irregularly distributed ones in planar near-field antenna measurements. In our technique we term 'The Cross-Rail Technique'; one dimensional (1-D) Yen interpolator is employed to reconstruct the two dimensional (2-D) uniform near-field data from the non-uniformly distributed samples. This approach extremely reduces the time complexity of interpolation algorithm, while the far-field pattern can yet be almost precisely predicted.

A comprehensive simulation capability has been developed and representative numerical results are presented. In order to assess the usefulness of the Cross-Rail technique, the speed and precision of Cross-Rail is compared to those of two other interpolation techniques, the Minimax technique [12] and the overlapping window technique [13]. Results so far indicate that the Cross-Rail technique is very powerful and can be used very advantageously for a variety of antenna pattern constructions from a set of non-uniform sampled points.

2. CROSS-RAIL TECHNIQUE

Yen's algorithm is an optimal (in the least square sense) band limited interpolation which is of great accuracy if being correctly used. According to Yen's algorithm, if E is a function band-limited to $\varnothing_{\max}$ and is non-uniformly sampled due to Nyquist rate, then E at any location in its domain can be exactly calculated by [14]

$$E(r) = \sum_{i=1}^{N} E(\xi_i)\Psi_i(r) \tag{1}$$

where N is the total number of sampled points and $\Psi_i(r)$ is the interpolation function chosen to be a combination of *Sinc* functions expressed as follows

$$\Psi_i(r) = \sum_{k=1}^{N} A_{ik} Sinc(\phi_{\max}(\xi_k - r)) \tag{2}$$

where

$$[A] = [C]^{-1} \tag{3}$$

and

$$C_{kj} = Sinc(w_{\max}(\xi_k - \xi_j)) \tag{4}$$

The above formulation can easily be expanded for two-dimensional cases, as well.

As pointed out earlier, if the quantity of samples increases, the computational complexity of Yen's algorithm extremely increases which makes this algorithm practically inefficient. Also, matrix $[C]$ in (4) is highly ill conditioned. This phenomenon aggravates as the size of matrix $[C]$ increase.

To overcome these problems, one may suggest setting $C_{kj} = 0$ for $k - j > M$ as in the Minimax interpolator [12]. This choice of $\{C_{kj}\}$ is reasonable since $[C]$ frequently has large elements on its diagonal, with relatively small off-diagonal elements that quickly decrease away from the diagonal. This process reduces the time complexity of the interpolation algorithm since it makes $[C]$ a sparse matrix.

Other may suggest using a $P \times P$ overlapping window with the desired point in the center [13]. This approach is also reasonable since each sample is highly correlated to its nearby samples.

The Cross-Rail technique is also based on the Yen's interpolator. While, the framework in Cross-Rail differs from the other techniques in which the Cross-Rail implements 1-D interpolators to 2-D signals. In Cross-Rail we assume that every 2-D signal band-limited to (ϕ_x, ϕ_z), consists of 1-D signals in either dimensions 'x' or 'z' that are band-limited to ϕ_x or ϕ_z, respectively. In other words, if we consider any plane parallel to, for example the 'yz' plane ($P : x = c$), the near-field pattern (which is spatially band-limited to (ϕ_x, ϕ_z)) will map a 1-D signal on P that is certainly band-limited to $\phi \leq \phi_z$.

As stated earlier, the near-field samples in a plane-rectangular sampling process, Fig. 1, may distribute non-uniformly on the scan plane due to probe position error as shown in Fig. 2. As a result the sample points will locate on/off the lines $L : x = c$ or $L : z = k$. Let us assume that the error in the position of probe does not exceed an upper bound of Δl as shown in Fig. 2.

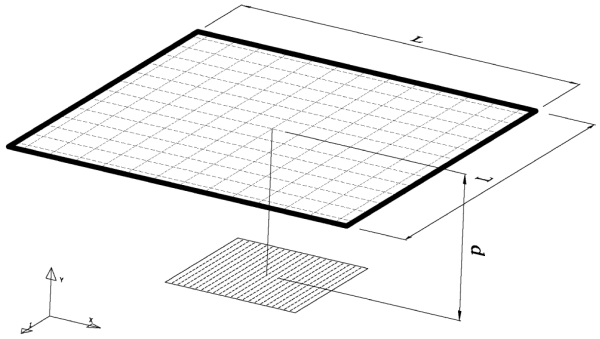

Figure 1. The plane-rectangular near-field scan plane located above an array of infinitesimal dipoles.

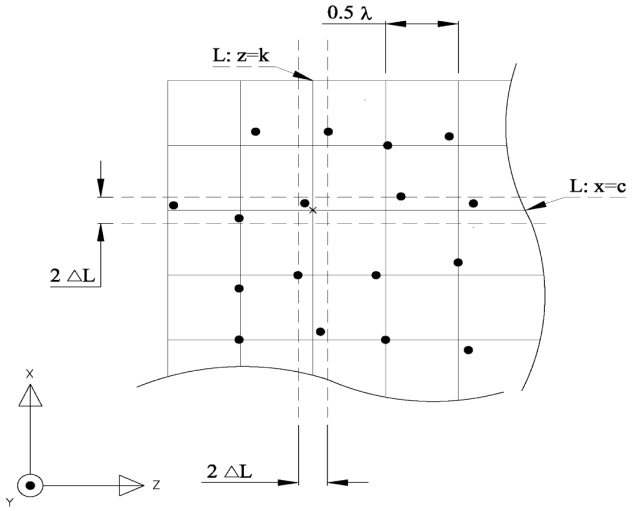

Figure 2. A representation of the Cross-Rail technique applied to non-uniformly distributed samples.

Also consider that $E_s(x_i, z_j)$ is the tangential component of the measured electric field at $(x_i = c,\ y = d, z_j)$. It can be seen from Fig. 3 that $z = z_j$ on $L : x = c$ is the closest point to $(x_i = c, z_j)$. Assuming $E_{app}(z_j)$ to be the tangential component of electric field at $(x = c,\ y = d, z_j)$. Since the radiated near-field is a spatially band-limited function of scan plane dimensions and $E_s(x_i, z_j)$ is just a fraction of wavelength away from $L : x = c$, we can approximately assume that the field intensity at $(x = c,\ y = d, z_j)$ equals $E_s(x_i, z_J)$.

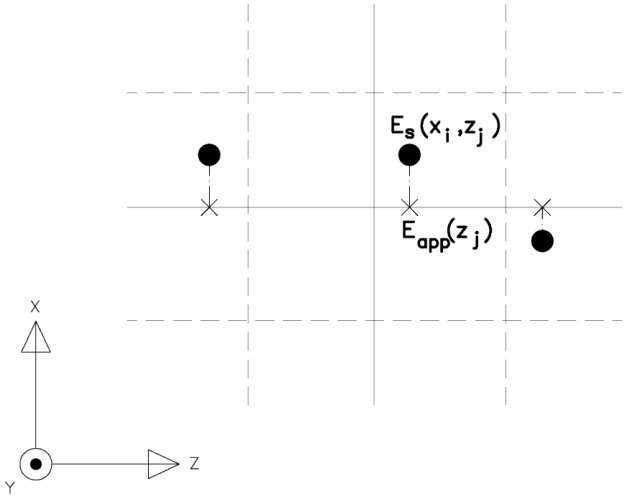

Figure 3. $E_{app}(z_j)$ is to be approximated by its nearby sample point $E_s(x_i, z_j)$.

In other words,

$$E_{app}(z_j) \cong E_s(x_i, z_j) \tag{5}$$

Therefore, the 1-D Yen interpolation algorithm can be deployed on non-uniformly spaced samples, $E_{app}(z_j)$, along $L : x = c$ in order to reconstruct the uniformly distributed data on the line.

Throughout this process, the Yen's interpolator is used to rearrange the sample points based on their correct locations in the direction of $L : x = c$ while, the differences between $E(c, z_j) = E_{app}(z_j)$ and $E_s(x_i, z_j)$ are neglected. The same process shall be repeated to rearrange the samples locating along $L : z = k$. As can be seen in Fig. 2, each point is to be reconstructed twice, once along a rail parallel to z axis and the other along a rail parallel to x axis. A linear combination of both estimations shall then define the field intensity at the intersection point.

As illustrated earlier, Cross-Rail is successful both for its good precision and its low computational complexity. Let us assume that the computational time complexity of Yen's interpolation algorithm is proportional to the time complexity of the inversion of matrix $[C]$ which is the most time taking part of the algorithm. Let us also assume that an aggregate number of $Q \times Q$ irregularly spaced samples are enclosed by Q parallel rails, each contains Q samples, as shown in Fig. 2.

The computational time complexity for direct implementing 2-

D Yen's algorithm to the above set of non-uniform samples is then proportional to $TC_d \approx Q^4 \log_2(Q^2)$ [15].

While, the time complexity of Cross-Rail technique (TC_{CR}) being implemented to the same set of data is proportional to

$$TC_{CR} \approx Q^3 \log_2(Q) \tag{6}$$

which is far less than TC_d.

Also, the ill condition phenomenon of the rather smaller $Q \times Q$ matrix $[C]$ as in the Cross-Rail technique is less than that of the $Q^2 \times Q^2$ matrix as in the 2-D Yen's algorithm which is of a great practical importance.

3. SIMULATION

A general and comprehensive simulation capability has been developed to compute the near and far field of an arbitrarily configured array of infinitesimal dipoles. Each dipole in the array can have a unique excitation, location, and orientation, as specified by its amplitude, Cartesian coordinates and Eulerian angles, respectively. The array far-field can be computed either by a direct summation, which produces an exact far-field pattern, or by computing the near-field using optimal interpolation sampling (OSI) techniques and processing the near-field data into the far-field using the FFT algorithm. This capability allows for direct comparison of the Cross-Rail technique, the overlapping window technique, the Minimax technique, and the exact far-field of the array.

In order to demonstrate the power of Cross-Rail technique, two different configuration of dipole arrays have been developed. The planar array under consideration is depicted in Fig. 4.

The first configuration is a low-gain dipole array consisting of 6 by 6 dipoles arranged on a half-wavelength-square lattice, creating an array with side dimensions of $D = 3$ wavelengths. All of the 36 dipoles are z-directed except for 6 randomly selected ones which have been rotated by a randomly selected angle between 0 and 90 degrees. The array elements also have excitations of different magnitude. The second configuration is a high-gain dipole array consisting 16 by 16 dipoles, also arranged on a half-wavelength-square lattice, creating an array with side dimensions of $D = 8$ wavelengths. All of the 256 dipoles are z-directed and have the same excitation and orientation.

The length of the scan plane, L, and the distance of the scan plane from the antenna under test (AUT), d, for the low-gain array and the high-gain array is set to be $L = 16\lambda,\ d = 2\lambda$ and $L = 24\lambda,\ d = 3\lambda$, respectively. This yields a valid angle of $\theta = 72$ degrees ($\sin(\theta) = 0.94$)

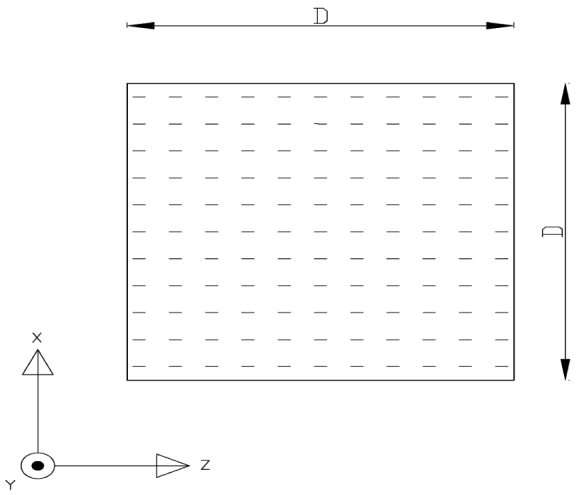

Figure 4. The simulated infinitesimal dipole array arranged on a half-wavelength-square lattice.

for both configurations. Also, the aggregate number of near-field samples for the low-gain and the high-gain arrays are 1089 and 2401 samples, respectively.

Figures 5 and 6 contain plots of the far-field E-plane co-polarized patterns of the low-gain and the high-gain arrays, respectively. Each figure includes two plots. One is the exact expression for the array's far-field and the other is the far-field computed through the NF to FF transformation of the uniform near-field samples that are reconstructed from the irregularly spaced measurements using the Cross-Rail technique. Agreement is seen to be excellent even to the side lobe levels of -60 dB in the high-gain array which has elements of uniform excitation and orientation. Also, for the low-gain array that contains elements with random excitation and orientation the results are satisfactory and show good agreement.

Fig. 7 demonstrates the normalized energy of error in the far-field of the high-gain dipole array for different values of maximum error in the position of probe ($2\Delta l$) calculated from Equation (7),

$$Error = \sum_{i=1}^{Q} \sum_{j=1}^{Q} \log[|E_{exact}| - |E_{int.}|] \tag{7}$$

where E_{exact} and $E_{int.}$ stand for the exact far-field and the far-field obtained from the OSI-FFT techniques, respectively. As can be seen

from Fig. 7, the rail width ($2\Delta l$) is assumed to change in the range of $[0.05\lambda, 0.25\lambda]$. The energy of error is computed for the Cross-Rail technique, the overlapping window technique ($p = 3, 5$), and the Minimax technique ($M = 1$). It should be noted that the energy of interpolation error in the near-field is also very similar to the energy of error in the far-field based on the Parsevals relation. Also, Table 1 shows the computation time complexity of the above mentioned techniques.

Table 1. The computational time complexity of the Minimax technique, the Overlapping window technique, and the Cross-Rail technique.

Technique	Minimax	Overlapping window		Cross-Rail
		(P=3)	(P=5)	
Time Complexity	$\leq Q^4 \log(Q^2)$	$\approx 9^2 \log(9) \times Q^2$	$\approx 25^2 \log(25) \times Q^2$	$\approx Q^3 \log(Q)$

It can be seen from Fig. 7 and Table 1 that the Minimax technique does neither give a good precision nor have a good time efficiency comparing to the other techniques. It should be noted that the precision of the Minimax interpolation technique might improve if larger integers were devoted to M which instead, would increase the computational time complexity of this technique.

The overlapping window technique gives relatively acceptable precision and low time complexity. A better precision will be obtained by enlarging the size of the overlapping window while a higher time complexity shall be tolerated in return.

The Cross-Rail technique, in comparison, enjoys both a good precision and a low time complexity. For example, for the case of 256-dipole array it can be seen from Table 1, that the time complexity of the Cross-Rail is at least one tenth of the time complexity of the overlapping window technique if a 5×5 window is deployed. However, it should be noted that the precision of the Cross-Rail is highly dependant on the upper bound of the probe position error. In other words, unlike the other two techniques, the precision of the Cross-Rail technique may not be simply improved. This poses limitations on the use of the Cross-Rail technique specifically in cases where the upper bound of error in the position of the measuring probe is not under control. But, for most applications with limited error in the position of the measuring probe the Cross-Rail is a fast, accurate and practical choice.

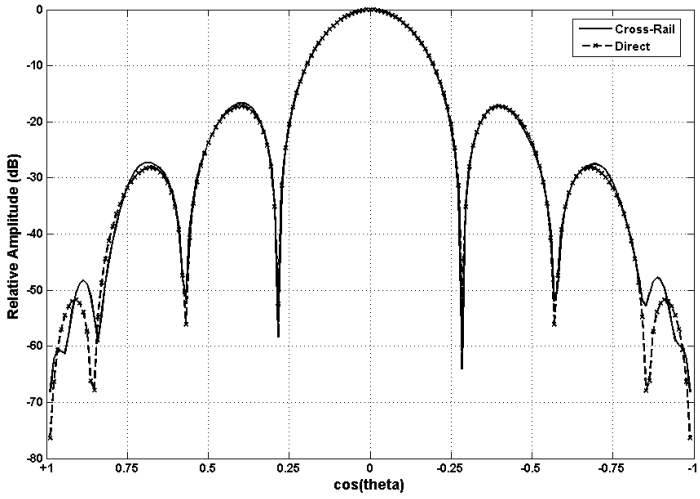

Figure 5. The E-plane co-polarized far-field pattern of the 36-element dipole array. The upper bound for error in the position of probe is set to be 0.1λ.

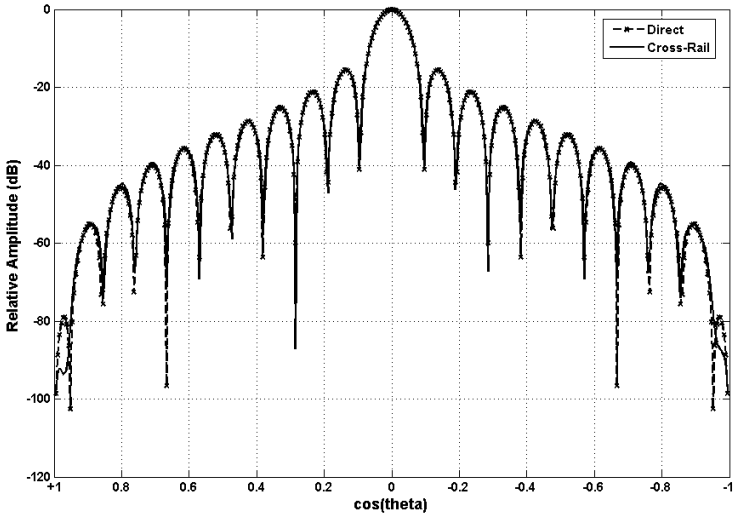

Figure 6. The E-plane co-polarized far-field pattern of the 256-element dipole array. The upper bound for error in the position of probe is set to be 0.1λ.

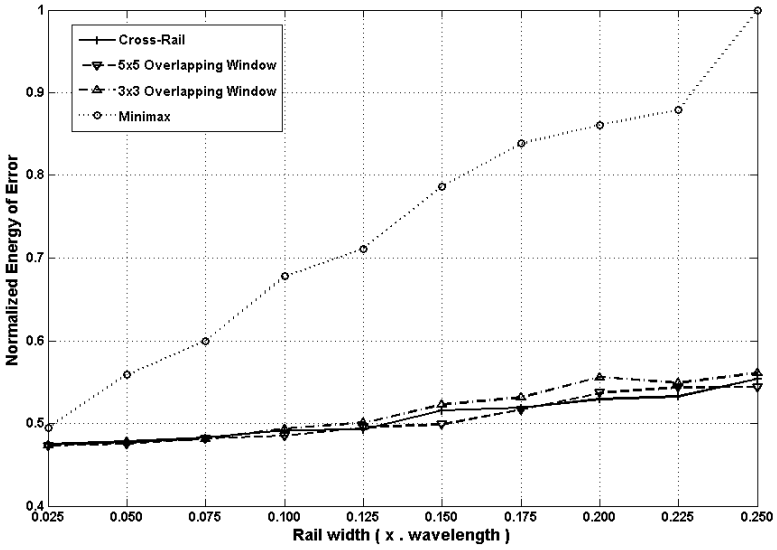

Figure 7. The normalized energy of error versus the rail-width ($2\Delta l$).

4. CONCLUSION

A new approach for the reconstruction of non-uniformly spaced planar near-field data is presented. It is shown through the simulations that this simple but highly efficient interpolation technique enjoys a very low computational time complexity and yet reconstructs the uniformly distributed near-field data with a good accuracy. The rearranged near-field data then was processed into the far-field and excellent agreement between the processed data and the exact far-field was obtained even for the side lobe level of -60 dB. It should be noted that in practice, the accuracy for far-field prediction through the use of planar-near-field scanners is limited to side lobe levels of 55–60 dB below the AUT's peak far-field as in the measurement facility of national institute of standard and technology, NIST, [16].

Simulations were conducted in order to evaluate the accuracy and the computational time complexity of Cross-Rail technique comparing to some other Yen based interpolation techniques. The results well demonstrate the performance and advantages of this fast, accurate and practically-interesting interpolation technique.

REFERENCES

1. Rahmat-Samii, Y., L. I. Williams, and R. G. Yaccarino, "The UCLA Bi-polar planar-near-field antenna measurement and diagnostics range," *IEEE Antennas and Propagation Magazine*, Vol. 42, No. 6, 16–35, 1995.
2. D'Agostino, F., C. Gennarelli, G. Riccio, and C. Savarese, "Theoretical foundations of near-field-far-field transformations with spiral scanning," *Progress In Electromagnetics Research*, PIER 61, 193–214, 2006.
3. Yaghjian, A. D., "An overview of near-field antenna measurements," *IEEE Transactions on Antennas and Propagation*, Vol. AP-34, No. 1, 30–45, 1986.
4. Newell, A. C., "Error Analysis Techniques for planar near-field measurements," *IEEE Transactions on Antennas and Propagation*, Vol. AP-36, No. 6, June 1988.
5. Fooshe, D. S., "Application of error correction technologies to near-field antenna measurement systems," *Proceedings of IEEE Aerospace Applications Conference*, Vol. 1,141–149, 1996.
6. Okhovvat, M. and M. Hakkak, "Probe-position error correction for time-domain planar near-field antenna measurements," *Iranian Journal of Science and Technology*, Vol. 26, 629–638, 2002.
7. Sten, J. C. and A. Hujanen, "Aspects on the phase delay and phase velocity in the electromagnetic near-field," *Progress In Electromagnetics Research*, PIER 56, 67–80, 2006.
8. Rahmat-Samii, Y. and R. Lap-Tung Cheung, "Nonuniform sampling techniques for antenna applications," *IEEE Transactions on Antennas and Propagation*, Vol. AP-35, No. 3, 268–279, 1987.
9. Jerri, A. J., "The Shannon sampling theorem -Its various extensions and applications: A tutorial review," *Proc. IEEE*, Vol. 65, No. 11, 1977.
10. Dehghanian, V., M. Okhovvat, and M. Hakkak, "A new interpolation method for reconstructing non-uniformly spaced samples into uniform ones in planar near-field antenna measurements," *IEEE Antennas and Propagation Society International Symposium*, Vol. 3, 207–210, 2003.
11. Bucci, O. M., C. Gennarelli, and C. Savarese, "Fast and accurate near-field-far-field transformation by sampling interpolation of plane polar measurements," *IEEE Transactions on Antennas and Propagation*, Vol. AP-39, 48–55, 1991.

12. Choi, H. and D. C. Munson, "Analysis and design of minimax-optimal interpolators," *IEEE Trans. Signal Processing*, Vol. 46, No. 6, 1998.
13. Ahmad, M. O., "An iterative procedure for uniform sampling of 2-D signals from non-equally spaced samples," *IEEE International Symposium on Circuits and Systems*, 1087–1091, 1989.
14. Yen, J. L., "On nonunifrom sampling of bandwidth-limited signals," *IEEE Trans. Circuit Theory*, Vol. CT-3, 251–257, 1956.
15. Raz, R., "On the complexity of matrix product," *SIAM Journal on Computing*, Vol. 32, No. 5, 1356–1369, 2003.
16. Francis, M. H., A. C. Newell, K. R. Grimm, J. Hoffman, and H. E. Schrank, "Comparison of ultra low sidelobe antenna for far field patterns using the planar near field method and the far field method," *IEEE Antenna and Propagation Magazine*, Vol. 37, No. 6, 1995.